

All optical 2-bit analog to digital converter using photonic crystal based cavities

Farhad Mehdizadeh¹  · Mohammad Soroosh¹ ·
Hamed Alipour-Banaei² · Ebrahim Farshidi¹

Received: 5 August 2016 / Accepted: 27 December 2016
© Springer Science+Business Media New York 2017

Abstract A novel design for realizing all optical analog to digital converter will be proposed in this paper. The proposed structure consists of two main parts; a nonlinear 3-channel demultiplexer, followed by an optical coder. The nonlinear demultiplexer will be used to quantize the input analog signal according to its optical intensity and the coder will convert the quantized levels into 2-bit binary codes. The nonlinear demultiplexer will be realized using three nonlinear resonant cavities. At appropriate values of input signal optical intensity one of the cavities can drop the optical beam to its corresponding output port. The proposed structure is capable of supporting maximum sampling rate up to 52 GS/s and total footprint of the structure is about 924 μm^2 .

Keywords Optical ADC · Photonic crystal · Kerr effect · Resonant cavity

1 Introduction

Photonic crystals (PhCs) are promising candidates for realizing all optical components suitable for implementing optical integrated circuits for present and future optical communications and signal processing systems. Due to existence of photonic band gap (Alipour-Banaei and Mehdizadeh 2013a; Diaz-Valencia and Calero 2014; Liu et al. 2015), which results from periodic modulation of refractive index, these artificial structures are capable of controlling the propagation of optical beams inside ultra-compact waveguides. Therefore so many optical components such as filters (Alipour-Banaei and Mehdizadeh 2013b; Djavid et al. 2008; Djavid and Abrishamian 2012; Ren et al. 2014; Robinson and

✉ Mohammad Soroosh
m.soroosh@scu.ac.ir

¹ Department of Electrical Engineering, Shahid Chamran University of Ahvaz, Ahvaz, Iran

² Department of Electronics, Tabriz Branch, Islamic Azad University, Tabriz, Iran

Nakkeeran 2013; Roshan Entezar 2015; Taalbi et al. 2013), demultiplexers (Alipour-Banaei et al. 2014b; Bernier et al. 2008; Bouamami and Naoum 2014; Jiu-Sheng et al. 2015; Khorshidahmad and Kirk 2010; Mansouri-Birjandi and Rakhshani 2013; Mehdizadeh and Soroosh 2015; Rostami et al. 2011), switches (Notomi et al. 2005; Teo et al. 2004; Wang et al. 2009; Zhang et al. 2007), logic gates and other logic devices (Alipour-Banaei et al. 2014a, c; Bao et al. 2014; Ghadrddan and Mansouri-Birjandi 2013; Goudarzi et al. 2016; Jiang et al. 2015; Jung et al. 2009; Liu et al. 2013; Mehdizadeh et al. 2015; Moniem 2015, 2016; Serajmohammadi et al. 2014) have been proposed based on PhC, whose dimensions are suitable for integration inside all optical circuits.

Electrical to optical and optical to electrical conversions inside optical networks expose mortal limitations of speed and bandwidth. Therefore all optical analog to digital converters (ADCs) are ultra-essential for high quality optical systems and networks. Recently few PhC based ADCs, have been proposed. Miao et al. (2006) proposed a 2-bit all optical ADC, which was composed of three cascaded optical beam splitters. These splitters have different splitting ratios. Youssefi et al. (2012) proposed another 2*bit ADC, by combining nonlinear Kerr effect with two cascaded high efficiency channel drop filter. Fasihi (Fasihi 2014) used three cascaded 3-dB optical power splitters, created inside 2D PhC to realize an all optical 2-bit ADC.

The fact is that none of above mentioned works perform the analog to digital conversion completely. All of them only produce quantized levels of input analog signal. But the produced codes are not well-defined standard binary codes. Most recently a 4-bit all optical ADC was proposed by Tavousi et al. (2016). In the proposed structure they employed nonlinear PhC ring resonators. Also they used two input ports for their structure which can limit the application of the proposed structure in all optical integrated circuits. The other drawback of the proposed structure is that they used four different refractive indices for the linear rods of the resonant ring, such that the average different between the refractive indices is about 0.02, realizing such a structure in real world is too difficult and complicated. In this paper we aim to solve this problem and propose a structure capable of producing standard binary codes from analog input signal. For this purpose we combined nonlinear demultiplexer, with an optical coder. The nonlinear demultiplexer performs the sampling and quantization and the coder produces a 2-bit binary standard code from the quantized levels obtained from the nonlinear demultiplexer.

In this paper we used plain wave expansion (PWE) and finite difference time domain (FDTD) methods for performing the required simulations and calculations. For obtaining accurate results, we used effective refractive index method to reduce 3D simulations into 2D simulations with acceptable accuracy. In this method in order to confine the optical beams in third dimensions the main material will be sandwiched between two layers of low refractive index such as SiO₂, for this method the refractive index of the material will be replaced by the effective index of guided modes in the 3D hetero-structure. Qiu (2002) explored and confirmed the validity of 2D approximation by the effective refractive index method.

The rest of the paper was organized as follows; in Sect. 2 we introduce the nonlinear 3-channel demultiplexer and its optical behavior, in Sect. 4 the final ADC and its functionality will be discussed and finally conclusions will be discussed in Sect. 4.

2 Nonlinear demultiplexer

As we know analog to digital conversion consists of three main steps; sampling, quantization and coding. In this paper the two first steps will be done with a nonlinear 3-channel demultiplexer, whose output ports should be controlled via optical intensity. The fundamental platform used for designing the nonlinear demultiplexer is a 2D square lattice array of dielectric rods. The fundamental platform has 40 rods in X direction and 46 in Z direction. Refractive index and radius of rods are $n = 3.46$ and $r = 0.26 \cdot a$, respectively where $a = 725$ nm is the lattice constant of the PhC. Using plane wave expansion (PWE) method (Johnson and Joannopoulos 2001) the band structure diagram of the fundamental structure was obtained like Fig. 1 which shows that the fundamental structure has two PBG regions in transverse magnetic (TM) mode (blue colored area). The second PBG region in TM mode is at $0.45 < a/\lambda < 0.54$ which is equal to $1342 \text{ nm} < \lambda < 1611 \text{ nm}$. Considering the PBG region the fundamental PhC is suitable for designing optical device in TM mode.

For creating the required demultiplexer we need one input and three output waveguides, which are created by removing dielectric rods from the appropriate locations and directions inside the fundamental PhC. Also for any output waveguide, there should be a wavelength

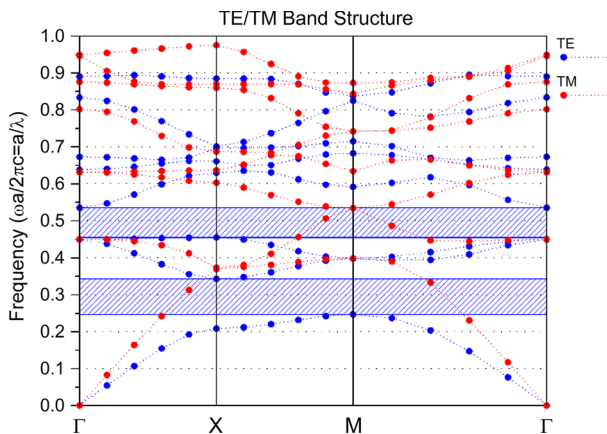


Fig. 1 The band structure of the fundamental platform

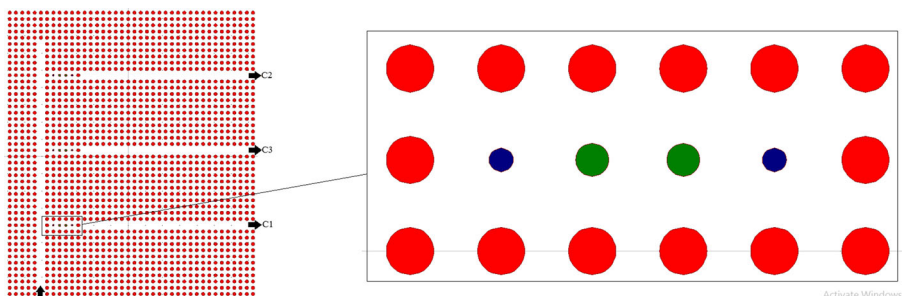


Fig. 2 Nonlinear demultiplexer along with resonant cavity

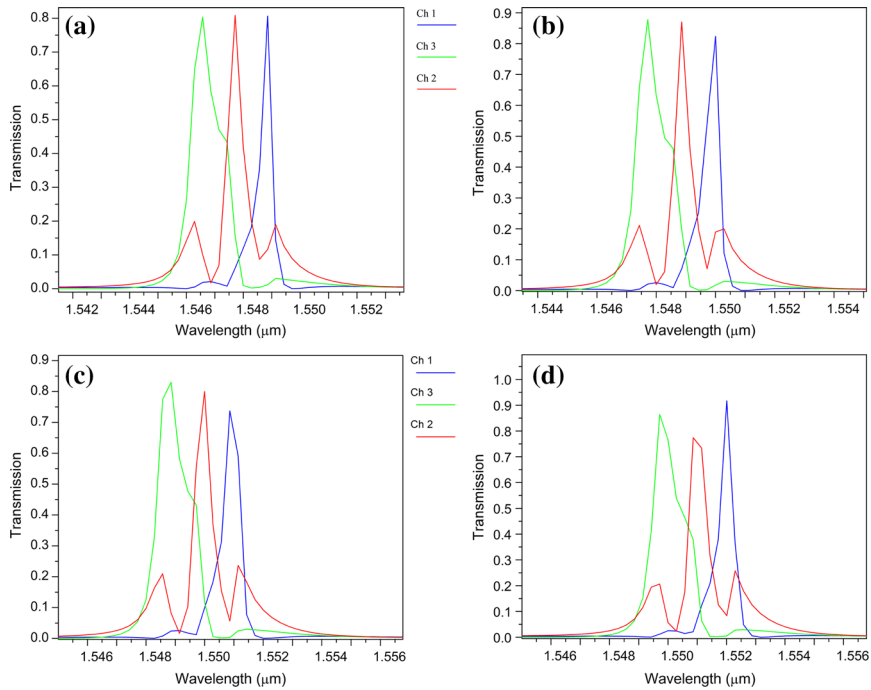


Fig. 3 Output spectra of the demultiplexer when the input power is at **a** $0 < P_{in} < 0.25P_0$, **b** $0.25P_0 < P_{in} < 0.5P_0$, **c** $0.5P_0 < P_{in} < 0.75P_0$ and **d** $0.75P_0 < P_{in} < P_0$

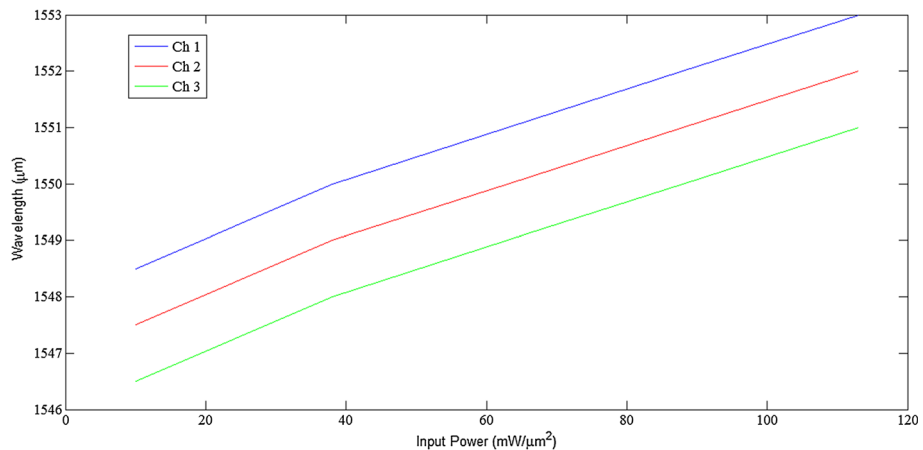


Fig. 4 Variation of resonant wavelengths of the output channels for different values of input power

selective structure, which was realized via resonant cavity in this paper. The resonant cavities consist of two corner and two inner defective rods. The radius of the corner defects was reduced in order to control the resonant mode and transmission efficiency of the resonant modes. Then for taking advantage of nonlinear Kerr effect and realizing a nonlinear demultiplexer whose output ports can be controlled via optical intensity, the inner

rods were replaced with dielectric rods made of doped glass, whose refractive index and nonlinear Kerr coefficient are $n_1 = 1.4$ and $n_2 = 10^{-14} \text{ m}^2/\text{W}$.

The nonlinear demultiplexer and its output spectra are shown in Fig. 2. The corner and inner defect rods are shown in blue and green respectively. The output spectra of the nonlinear demultiplexer for different values of input power are shown in Fig. 3. As shown in Fig. 3a, the nonlinear demultiplexer has three resonant modes. When the input power is at $0 < P_{\text{in}} < 0.25P_0$ range, these resonant modes are at $\lambda_1 = 1548.5 \text{ nm}$, $\lambda_2 = 1547.5 \text{ nm}$, and $\lambda_3 = 1546.5 \text{ nm}$ for the first, second and third output ports, respectively. However by increasing the input power the resonant modes shift toward higher wavelengths (as shown

Table 1 Normalized output power of the nonlinear demultiplexer for different values of the optical intensity

P_{in}	Ch 1 (%)	Ch 2 (%)	Ch 3 (%)
$0 < P_{\text{in}} < 0.25P_0$	2	2	1
$0.25P_0 < P_{\text{in}} < 0.5P_0$	80	5	2
$0.5P_0 < P_{\text{in}} < 0.75P_0$	5	75	2
$0.75P_0 < P_{\text{in}} < P_0$	3	5	75

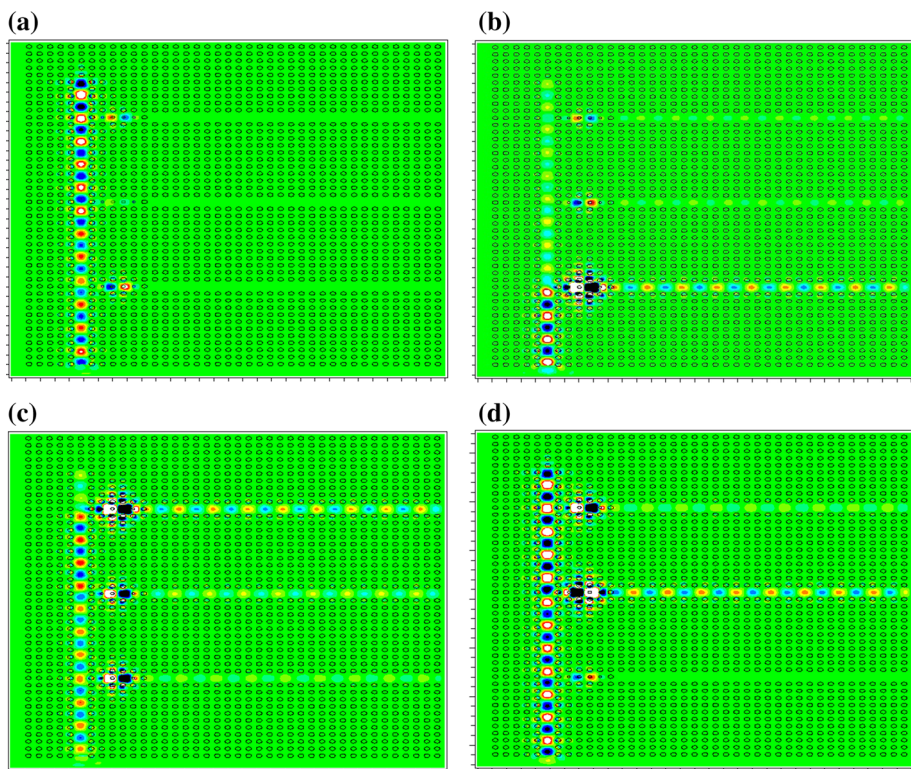


Fig. 5 Optical behavior of the nonlinear demultiplexer for the optical intensity being at **a** $0 < P_{\text{in}} < 0.25P_0$, **b** $0.25P_0 < P_{\text{in}} < 0.5P_0$, **c** $0.5P_0 < P_{\text{in}} < 0.75P_0$ and **d** $0.75P_0 < P_{\text{in}} < P_0$

in Figs. 3, 4). The central wavelength of the resonant modes of output ports for different values of input power are listed in Table 1.

An optical beam via central wavelength of 1550 nm and optical intensity (P_{in}) less than $P_0 = 0.1 \text{ W}/\mu\text{m}^2$ was used for simulating the nonlinear demultiplexer. Due to existence of nonlinear rods, the functionality of the structure strongly depends on input optical intensity. When the optical intensity is at $0 < P_{in} < 0.25P_0$, the central wavelength of the input beam coincides with none of the resonant cavities, so none of the cavities will drop the optical beam from input port into their corresponding output waveguides and the normalized power at all output ports will be less than 5% (Fig. 6a). Therefore all the output ports will be OFF (Fig. 5a). Increasing the input optical intensity increases the refractive index of inner rods, which results in blue shift in the resonant wavelength of the cavities. When the input optical intensity is about $0.25P_0 < P_{in} < 0.5P_0$, the resonant mode of the first cavity coincides with the central wavelength of input beam, so it will drop the optical beam into the first output waveguide and Ch#1 will be on (Fig. 5b). In this case the normalized power at Ch#1, Ch#2 and Ch#3 will be 80, 5 and 2% respectively (Fig. 6b). Similarly When the input optical intensity is about $0.5P_0 < P_{in} < 0.75P_0$, the resonant mode of the second cavity coincides with the central wavelength of input beam, so it will drop the optical beam into the second output waveguide and Ch#2 will be on (Fig. 5c). In this case the normalized power at Ch#1, Ch#2 and Ch#3 will be 5, 75 and 2% respectively (Fig. 6c). Finally When the input optical intensity is about $0.75P_0 < P_{in} < P_0$, the resonant mode of the third cavity coincides with the central wavelength of input beam, so it will drop the optical beam into the third output waveguide and Ch#3 will be on (Fig. 5d). In this

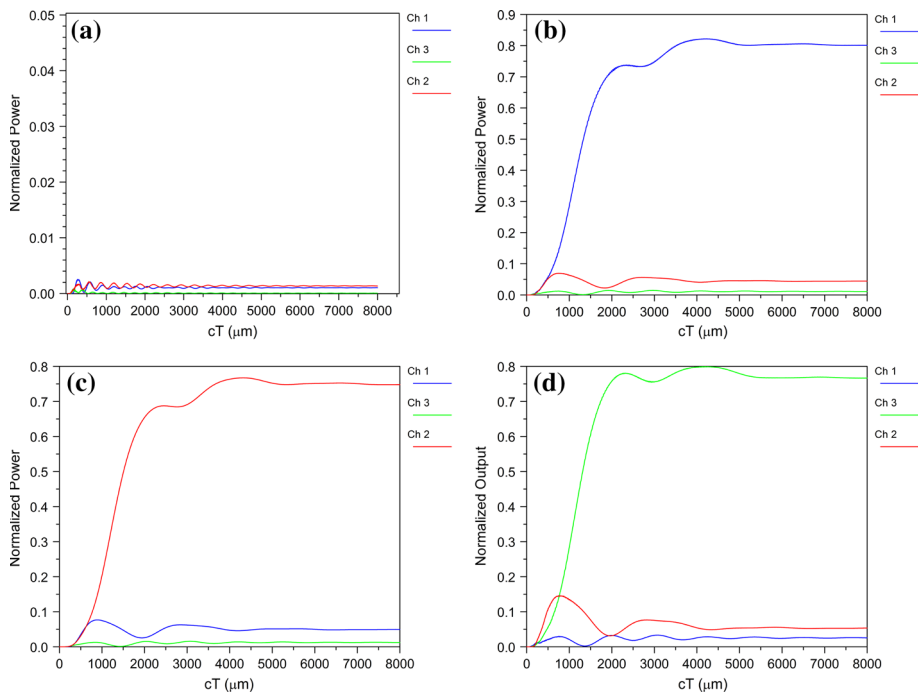


Fig. 6 Normalized output power of the nonlinear demultiplexer for the optical intensity being at **a** $0 < P_{in} < 0.25P_0$, **b** $0.25P_0 < P_{in} < 0.5P_0$, **c** $0.5P_0 < P_{in} < 0.75P_0$ and **d** $0.75P_0 < P_{in} < P_0$

case the normalized power at Ch#1, Ch#2 and Ch#3 will be 3, 5 and 75% respectively (Fig. 6b). As one can see the maximum normalized power for Ch#1, Ch#2 and Ch#3 at ON states are 80, 75 and 75% respectively. Also the maximum normalized power for Ch#1, Ch#2 and Ch#3 at OFF states are 5%. Therefore the ratio of OFF optical power level to ON optical power level for Ch#1, Ch#2 and Ch#3 will be 6.25, 6.7 and 6.7% respectively.

3 All optical ADC

Now for completing the analog to digital conversion and realizing the final ADC, we should add a section which can convert the quantized levels to 2-bit binary code. The coder section was realized by creating some additional waveguides inside the structure. The final sketch of the proposed 2-bit ADC is shown in Fig. 7.

The total structure has one input and two output ports. O1 is representative of the least significant bit (LSB), and O2 is representative of the most significant bit (MSB). Between input waveguide and output waveguides there are three resonant cavities and some intermediate waveguides. W1 is the input and W2 and W3 are the output waveguides. W4, W6 and W5 correspond to the first, second and third resonant cavities respectively. W6 was split to two parts via a T-shaped splitter. The resulted splitter has two branches labeled W7 and W8. W7 joins W4 at the front side of W2, also W8 joins W5 at the front side of W3. Therefore the required optical paces will be created between the input port and output ports. At the following we are going to investigate the functionality of the proposed structure.

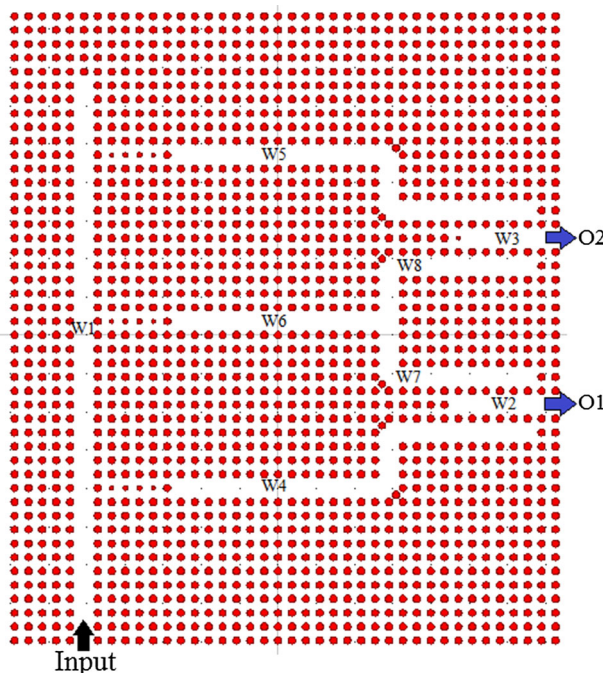


Fig. 7 The final sketch of the proposed ADC

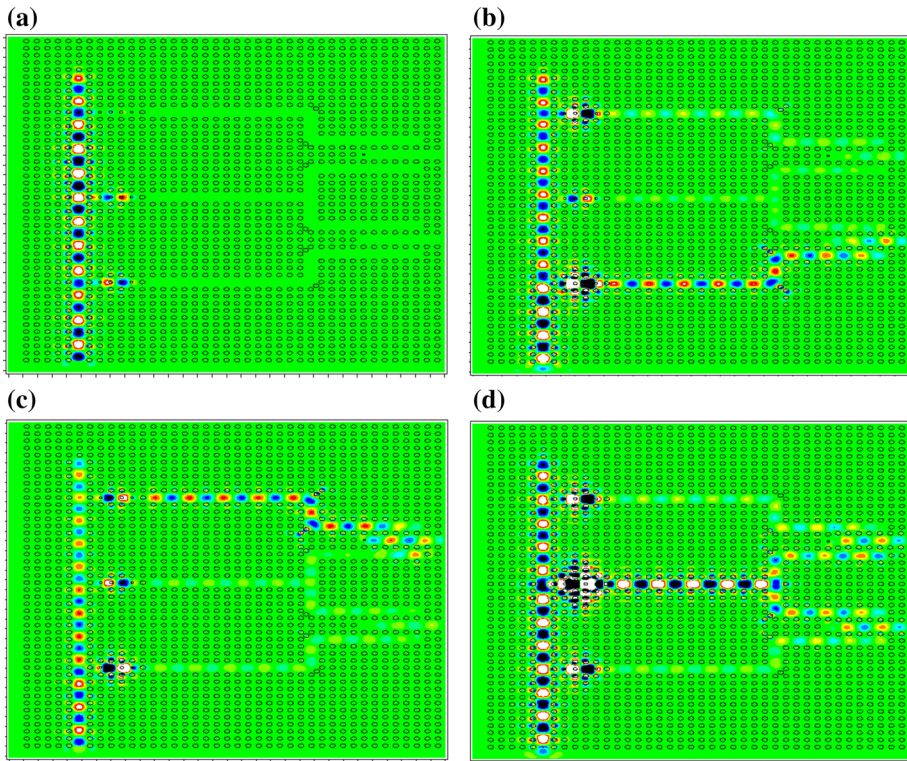


Fig. 8 Optical behavior of the proposed optical ADC for the optical intensity being at **a** $0 < P_{in} < 0.25P_0$, **b** $0.25P_0 < P_{in} < 0.5P_0$, **c** $0.5P_0 < P_{in} < 0.75P_0$ and **d** $0.75P_0 < P_{in} < P_0$

The proposed structure is a 2-bit optical ADC, so there should be four different working states corresponding to four different ranges for the input optical intensity. In this paper the, for the output ports optical intensity more than $0.25P_0$ ($P_0 = 0.1 \text{ W}/\mu\text{m}^2$) considered as logic 1 and optical intensity less the $0.05P_0$ considered as logic 0. When the input signal optical intensity is at $0 < P_{in} < 0.25P_0$ ($P_0 = 0.1 \text{ W}/\mu\text{m}^2$), none of the resonant cavities would couple the optical beam from input port to their corresponding output waveguides. So both of the output ports will be OFF and the generated code will be “00” (Fig. 8a).

For P_{in} at $0.25P_0 < P_{in} < 0.5P_0$, only the first cavity will drop the optical beam from W1 into W4. The dropped beam finds its way toward O1 through W4 and W7. So O1 will be on and O2 will be OFF, and the generated code will be “01” (Fig. 8b). For P_{in} at $0.5P_0 < P_{in} < 0.75P_0$, only the second cavity will drop the optical beam from W1 into W5. The dropped beam finds its way toward O2 through W5 and W8. So O2 will be on and O1 will be OFF, and the generated code will be “10” (Fig. 8c). Finally when P_{in} is at $0.75P_0 < P_{in} < P_0$, only the third cavity will drop the optical beam from W1 into W6. The dropped beam finds its way toward O1 and O2 through W5, W7 and W8. So O1 and O2 will be on, and the generated code will be “11” (Fig. 8d). These states were summarized in Table 2.

As shown we proposed an all optical 2-bit analog to digital converter which is capable of generating standard 2-bit binary codes from the optical intensity of the input analog signal. Time response of the structure for the third case is shown in Fig. 9. As shown in

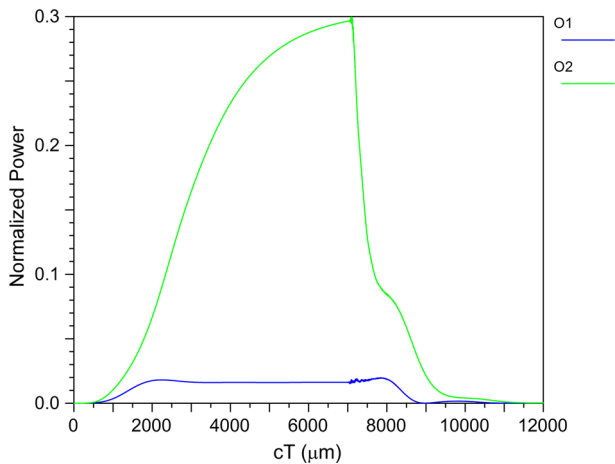


Fig. 9 Time response of the structure used for calculating the delay times

Table 2 Working states of the proposed ADC

P_{in}	O2	O1
$0 < P_{in} < 0.25P_0$	0	0
$0.25P_0 < P_{in} < 0.5P_0$	0	1
$0.5P_0 < P_{in} < 0.75P_0$	1	0
$0.75P_0 < P_{in} < P_0$	1	1

Fig. 9, the maximum time required for the O2 output port to reach $0.25P_0$ is about $cT = 4200 \mu\text{m}$, for converting this value to standard time we should divide it by $c = 3 \times 10^8 \text{ m/s}$, there for the maximum time required for O2 to reach $0.25 P_0$ is about 14 ps. In order to obtain the shut off delay we turned off the source at $cT = 700 \mu\text{m}$, Fig. 9 shows that at $cT = 8560 \mu\text{m}$ the output power declines to $0.05 P_0$, so the maximum shut off time is about $cT = 1560 \mu\text{m}$. If we divide this value by $c = 3 \times 10^8 \text{ m/s}$, the maximum time required for the O2 output port to reach $0.05P_0$ when the source is OFF, will be about 5.2 ps, so the minimum time period for the input pulse should be more than 19.2 ps. Therefore the maximum sampling rate will be about 52 GS/s. Total footprint of the proposed optical ADC is about $924 \mu\text{m}^2$.

4 Conclusion

In this paper an all optical analog to digital converter was proposed based on nonlinear resonant cavities. The proposed structure has one input and two output ports, which generates 2-bit binary codes from the optical input signal. A nonlinear 3-channel demultiplexer was used to quantize the optical intensity of the input signal, then an optical coder was used to convert the quantized levels into 2-bit binary codes. Maximum sampling rate and total foot print of the structure are about 52 GS/s and $924 \mu\text{m}^2$ respectively.

References

- Alipour-Banaei, H., Mehdizadeh, F.: Bandgap calculation of 2D hexagonal photonic crystal structures based on regression analysis. *J. Opt. Commun.* **34**, 285–293 (2013a)
- Alipour-Banaei, H., Mehdizadeh, F.: Significant role of photonic crystal resonant cavities in WDM and DWDM communication tunable filters. *Opt. Int. J. Light Electron Opt.* **124**, 2639–2644 (2013b)
- Alipour-Banaei, H., Mehdizadeh, F., Serajmohammadi, S., Hassangholizadeh-Kashtiban, M.: A 2*4 all optical decoder switch based on photonic crystal ring resonators. *J. Mod. Opt.* **62**, 430–434 (2014a)
- Alipour-Banaei, H., Serajmohammadi, S., Mehdizadeh, F.: Optical wavelength demultiplexer based on photonic crystal ring resonators. *Photonic Netw. Commun.* **29**, 146–150 (2014b)
- Alipour-Banaei, H., Serajmohammadi, S., Mehdizadeh, F.: All optical NOR and NAND gate based on nonlinear photonic crystal ring resonators. *Opt. Int. J. Light Electron Opt.* **125**, 5701–5704 (2014c)
- Bao, J., Xiao, J., Fan, L., Li, X., Hai, Y., Zhang, T., Yang, C.: All-optical NOR and NAND gates based on photonic crystal ring resonator. *Opt. Commun.* **329**, 109–112 (2014)
- Bernier, D., Le Roux, X., Lupu, A., Marris-Morini, D., Vivien, L., Cassan, E.: Compact, low cross-talk CWDM demultiplexer using photonic crystal superprism. *Opt. Express* **16**, 17209–17214 (2008)
- Bouamami, S., Naoum, R.: New version of seven wavelengths demultiplexer based on the microcavities in a two-dimensional photonic crystal. *Opt. (Stuttg.)* **125**, 7072–7074 (2014)
- Diaz-Valencia, B.F., Calero, J.M.: Photonic band gaps of a two-dimensional square lattice composed by superconducting hollow rods. *Phys. C Supercond.* **505**, 74–79 (2014)
- Djavid, M., Abrishamian, M.S.: Multi-channel drop filters using photonic crystal ring resonators. *Opt. Int. J. Light Electron Opt.* **123**, 167–170 (2012)
- Djavid, M., Ghaffari, A., Monifi, F., Abrishamian, M.S.: T-shaped channel-drop filters using photonic crystal ring resonators. *Phys. E Low Dimens. Syst. Nanostruct.* **40**, 3151–3154 (2008)
- Fashti, K.: All-optical analog-to-digital converters based on cascaded 3-dB power splitters in 2D photonic crystals. *Opt. Int. J. Light Electron Opt.* **125**, 6520–6523 (2014)
- Ghadrdan, M., Mansouri-Birjandi, M.A.: Concurrent implementation of all-optical half-adder and AND & XOR logic gates based on nonlinear photonic crystal. *Opt. Quantum Electron.* **45**, 1027–1036 (2013)
- Goudarzi, K., Mir, A., Chaharmahali, I., Goudarzi, D.: All-optical XOR and OR logic gates based on line and point defects in 2-D photonic crystal. *Opt. Laser Technol.* **78**, 139–142 (2016)
- Jiang, Y.-C., Liu, S.-B., Zhang, H.-F., Kong, X.-K.: Realization of all optical half-adder based on self-collimated beams by two-dimensional photonic crystals. *Opt. Commun.* **348**, 90–94 (2015)
- Jiu-Sheng, L., Han, L., Le, Z.: Compact four-channel terahertz demultiplexer based on directional coupling photonic crystal. *Opt. Commun.* **350**, 248–251 (2015)
- Johnson, S., Joannopoulos, J.: Block-iterative frequency-domain methods for Maxwell's equations in a planewave basis. *Opt. Express* **8**, 173–190 (2001)
- Jung, Y.J., Yu, S., Koo, S., Yu, H., Han, S., Park, N., Kim, J.H., Jhon, Y.M., Lee, S.: Reconfigurable all-optical logic AND, NAND, OR, NOR, XOR and XNOR gates implemented by photonic crystal nonlinear cavities. In: Conference on Lasers and Electro-Optics/Pacific Rim. p. TuB4_3. Optical Society of America (2009)
- Khorshid Ahmad, A., Kirk, A.G.: Composite superprism photonic crystal demultiplexer: analysis and design. *Opt. Express* **18**, 20518–20528 (2010)
- Liu, D., Gao, Y., Tong, A., Hu, S.: Absolute photonic band gap in 2D honeycomb annular photonic crystals. *Phys. Lett. A* **379**, 214–217 (2015)
- Liu, W., Yang, D., Shen, G., Tian, H., Ji, Y.: Design of ultra compact all-optical XOR, XNOR, NAND and OR gates using photonic crystal multi-mode interference waveguides. *Opt. Laser Technol.* **50**, 55–64 (2013)
- Mansouri-Birjandi, M.A., Rakhshani, M.R.: A new design of tunable four-port wavelength demultiplexer by photonic crystal ring resonators. *Opt. Int. J. Light Electron Opt.* **124**, 5923–5926 (2013)
- Mehdizadeh, F., Soroosh, M.: A new proposal for eight-channel optical demultiplexer based on photonic crystal resonant cavities. *Photonic Netw. Commun.* **31**, 65–70 (2015)
- Mehdizadeh, F., Soroosh, M., Alipour-Banaei, H.: A novel proposal for optical decoder switch based on photonic crystal ring resonators. *Opt. Quantum Electron.* **48**, 20–28 (2015)
- Miao, B., Chen, C., Sharkway, A., Shi, S., Prather, D.W.: Two bit optical analog-to-digital converter based on photonic crystals. *Opt. Express* **14**, 7966–7973 (2006)
- Moniem, T.A.: All optical active high decoder using integrated 2D square lattice photonic crystals. *J. Mod. Opt.* **62**, 1643–1649 (2015)
- Moniem, T.A.: All-optical digital 4 × 2 encoder based on 2D photonic crystal ring resonators. *J. Mod. Opt.* **63**, 735–741 (2016)

- Notomi, M., Shinya, A., Mitsugi, S., Kira, G., Kuramochi, E., Tanabe, T.: Optical bistable switching action of Si high-Q photonic-crystal nanocavities. *Opt. Express* **13**, 2678–2687 (2005)
- Qiu, M.: Effective index method for heterostructure-slab-waveguide-based two-dimensional photonic crystals. *Appl. Phys. Lett.* **81**, 1163–1165 (2002)
- Ren, C., Wang, P., Cheng, L., Feng, S., Gan, L., Li, Z.: Multichannel W3 Y-branch filter in a two dimensional triangular-lattice photonic crystal slab. *Opt. Int. J. Light Electron Opt.* **125**, 7203–7206 (2014)
- Robinson, S., Nakkeeran, R.: Two dimensional photonic crystal ring resonator based add drop filter for CWDM systems. *Opt. Int. J. Light Electron Opt.* **124**, 3430–3435 (2013)
- Roshan Entezar, S.: Photonic crystal wedge as a tunable multichannel filter. *Superlattices Microstruct.* **82**, 33–39 (2015)
- Rostami, A., Banaei, H.A., Nazari, F., Bahrami, A.: An ultra compact photonic crystal wavelength division demultiplexer using resonance cavities in a modified Y-branch structure. *Opt. Int. J. Light Electron Opt.* **122**, 1481–1485 (2011)
- Serajmohammadi, S., Alipour-Banaei, H., Mehdizadeh, F.: All optical decoder switch based on photonic crystal ring resonators. *Opt. Quantum Electron.* **47**, 1109–1115 (2014)
- Taalbi, A., Bassou, G., Youcef Mahmoud, M.: New design of channel drop filters based on photonic crystal ring resonators. *Opt. Int. J. Light Electron Opt.* **124**, 824–827 (2013)
- Tavousi, A., Mansouri-Birjandi, M.A., Saffari, M.: Successive approximation-like 4-bit full-optical analog-to-digital converter based on Kerr-like nonlinear photonic crystal ring resonators. *Phys. E Low-dimens. Syst. Nanostruct.* **83**, 101–106 (2016)
- Teo, H.G., Liu, A.Q., Singh, J., Yu, M.B., Bourouina, T.: Design and simulation of MEMS optical switch using photonic bandgap crystal. *Microsyst. Technol.* **10**, 400–406 (2004)
- Wang, T., Li, Q., Gao, D.: Ultrafast polarization optical switch constructed from one-dimensional photonic crystal and its performance analysis. *Chin. Sci. Bull.* **54**, 3663–3669 (2009)
- Youssefi, B., Moravvej-Farshi, M.K., Granpayeh, N.: Two bit all-optical analog-to-digital converter based on nonlinear Kerr effect in 2D photonic crystals. *Opt. Commun.* **285**, 3228–3233 (2012)
- Zhang, Y., Zhang, Y., Li, B.: Optical switches and logic gates based on self-collimated beams in two-dimensional photonic crystals. *Opt. Express* **15**, 9287–9292 (2007)